

the polymer. X rays and electrons do not produce tracks in CN. Hydrogenic ions are capable of producing only short ($< 6 \mu\text{m}$) ionization tracks in CN. Such tracks are *not* transformed into pinholes passing *all the way through* the CN layer by the etch procedures. Thus, the pinhole array recorded in the polymer detector (Fig. 1) is in fact representative of the spatial distribution of α particles incident on the CN film.

¹⁷N. M. Ceglio, "Zone Plate Coded Imaging of Alpha Particle Emission from Laser Fusion Targets" Lawrence Livermore Laboratory, Laser Program Annual

Report, 1976 (unpublished), Article I.B.3i.

¹⁸J. T. Larsen, Bull. Am. Phys. Soc. **20**, 1267 (1975).

¹⁹The FWHM dimensions of the central region of the compressed target taken from x-ray microscopic images (at $\sim 4 \text{ keV}$) of the imploded shell are ($32 \mu\text{m}$, $31 \mu\text{m}$) for shot A and ($40 \mu\text{m}$, $32 \mu\text{m}$) for shot B along the vertical and horizontal axes respectively. The agreement between the eccentricities measured from FWHM α imaging data and FWHM x-ray imaging data is within experimental uncertainty, and illustrates the similarity in shape of the two types of images

Geometric Focusing of 20-GW Proton Beams with Use of a Magnetically Insulated Diode

M. Greenspan, S. Humphries, Jr., J. Maenchen, and R. N. Sudan

Laboratory of Plasma Studies, Cornell University, Ithaca, New York 14853

(Received 14 March 1977)

We have obtained initial geometric-focusing results using a high-current ($\geq 100 \text{ kA}$) magnetically insulated diode. At the line focus, current densities over 300 A/cm^2 have been obtained with a radial compression of about 10. Results for propagation of the intense beams are in excellent agreement with geometric single-particle predictions.

Studies of the propagation of proton beams produced by a high-power, magnetically insulated diode ($> 100 \text{ kA}$ at up to 300 kV) are described in this Letter. The diode is a major scale-up of previous work.¹ The chief developments in the present experiment were the following: (a) An order-of-magnitude increase in current output was achieved over that previously reported for magnetically insulated diodes^{1,2} while preserving the virtues of high efficiency and low electrode damage. (b) An extraction cathode of thickness larger than the skin depth for the pulsed insulating magnetic field was used so that the field was confined to the anode-cathode gap. Thus the region interior to the cylindrical cathode was field-free and the beam propagates with minimum magnetic deflection. (c) The propagation of ion beams through vacuum with cold electron neutralization was studied in a region well shielded from diode effects. (d) High ion-current densities, in excellent agreement with geometric predictions, were obtained at the focus.

Maximization of the ion-beam power density is of particular interest in relation to proposals for ion-beam-induced pellet fusion.³⁻⁵ Although, for ease of construction, the diode described was designed to produce a line focus, magnetically insulated diodes have potential for producing spherically converging beams, either with a single acceleration gap¹ or in a stacked configuration.

The experimental system is shown in Fig. 1. The goal was to design a high-current diode at

medium voltage to take advantage of the low-impedance output from the Neptune C generator.⁶ The geometry is cylindrical, with ions extracted inwards. The cylindrical cathode with slot extractors has an L/R time long compared to the magnetic-field risetime and thus excludes the field from the inner propagation volume, allowing the ions to approach closer to the axis. The

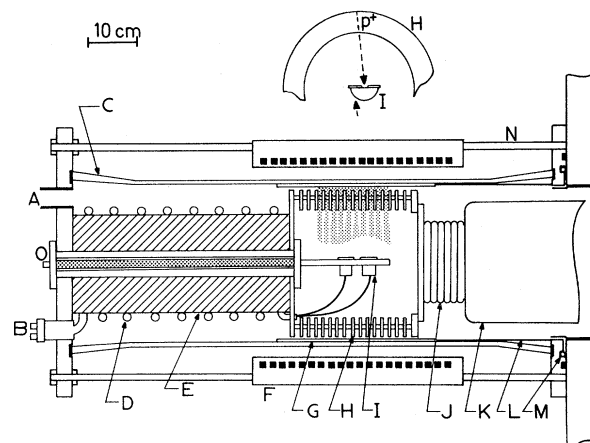


FIG. 1. Experimental apparatus: A, pumping port; B, diagnostic isolator output; C, glass vacuum vessel, 30 cm i.d.; D, diagnostic isolation inductor; E, Delrin support rod; F, 20-turn, 20-kG magnetic coil; G, anode; H, cathode assembly; I, ion-current-density probes; J, bellows for electrical connection; K, high-voltage terminal from the Neptune C generator; L, return conductors; M, Rogowski loop-current monitor; N, support rods; O, resistive diode-voltage monitor.

exclusion electrode also maintains field-line parallelism in the acceleration gap, and produces a magnetic-field-line curvature at the ends to prevent axial electron losses. The diode had to be located some distance from the heavy aluminum flange of the Neptune C generator in order to avoid excessive mechanical stress from the magnetic field. To minimize inductance, the center electrode was pulsed negative to pull protons inward. Even so, there was a total diode inductance of about 60 nH so that it was not possible to use the generator at optimum efficiency.

The outer anode (of radius 15 cm) was a slotted stainless-steel sheet on which anodes with plasmas produced by surface breakdowns of 500 to 2000 cm² could be mounted.⁷ The cathode was constructed of stacked aluminum disks and had about a 50% transparency. The ultimate goal was to use this in conjunction with a localized plasma source¹ to produce ion beams only at the slots, but, for convenience in this initial run, a general-area source was used. Gap spacing was maintained at 0.6 cm. The diode impedance could be adjusted by changing the axial length of the plasma anode.

Since the propagation volume was pulsed to high voltage, time-resolved diagnostics inside the cathode were performed with use of the isolation inductor shown in Fig. 1, which carried four coaxial cables. There was less than 1 V of residual noise on the detectors from the 300-kV pulse. Standard biased charge collectors,⁸ as well as special charge collectors designed to measure beams of large axial divergence (e.g., at the focus), gave time-resolved measurements of ion current density. These compared well at the periphery with calorimeter measurements. Witness plates gave very graphic indications of beam-divergence and -focusing properties. Magnetic insulation tests were first performed using a bare metal anode. The absence of signals from the ion probes showed there were no crossing ions in this case. In order to prevent electron flow effectively, field lines must be parallel to the accelerating gap. In the large-area diode in question, this meant an alignment accuracy of better than 1°. With the field-exclusion cathode, this was not a concern, since field lines are automatically constrained to be parallel to the cathode surface (with some small-scale bulging into the slots). Magnetic-insulation results are shown in Fig. 2. The perveance at high values of the ratio of the magnetic field to the critical value (B^*) is reduced by a factor of 170 from the

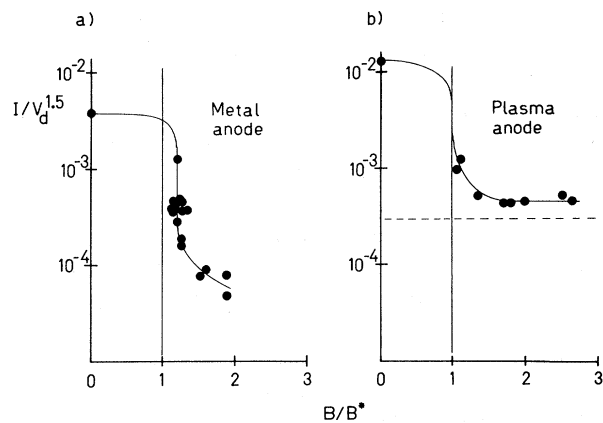


FIG. 2. Perveance measurements at 50 nsec, as a function of B/B^* . (a) 2000-cm² aluminum anode; (b) 1100-cm² plasma anode. All quantities calculated for $d = 0.43$ cm. Horizontal dotted line is Child-Langmuir proton perveance.

Child-Langmuir electron value. This indicates excellent parallelism and axial electron confinement. The 20% deviation of the break in the curve from $B/B^* = 1$ could be due to a combination of slight misalignment of the anode-cathode gap and diode closure. The perveance behavior changes markedly when a plasma anode is used, as in Fig. 2(b). Instead of decreasing with high B/B^* , the perveance saturates, in agreement with the prediction that the ion current density is close to the Child-Langmuir prediction when $B > 1.5B^*$.^{9,10} In order to analyze the data, the acceleration-gap spacing must be known. Ion-current-density measurements indicate that at 50 nsec from the initiation of the voltage pulse, diode closure from the plasma anode has reduced the initial gap to 0.43 ± 0.04 cm. The use of this value to compute B^* gives the plot shown. The Child-Langmuir proton perveance for this gap spacing is also shown. This indicates that the proton current is about 66% of the total current.

Theoretically, this diode should produce an ion current close to the Child-Langmuir in a well-insulated regime.^{9,10} Since the diode self-magnetic-field (B_θ) is typically less than 5% of the applied field, electron drifts are approximately continuous and there should be no enhancement effects from electron space-charge compression.¹¹ The proton current density could be measured by probes inside the cathode at the 10-cm radius and the current density at the cathode radius (14 cm) inferred by dividing by 1.4. On a shot to shot basis, the response of a particular probe is very

consistent, but there is about a $\pm 50\%$ variation with axial and azimuthal position. This is probably due to the relatively coarse nature of the plasma anode which affects plasma closure rates locally. Witness plates indicate variations of energy deposition on a scale size corresponding to the capacitive division⁷ of the plasma anode. Even so, to achieve this degree of uniformity required some effort. The anode (consisting of 0.3-cm-thick polyethylene punctured by flush pins in line with the slots with about 1-cm azimuthal spacing) was divided into over 2000 capacitive elements. Fortunately, such anodes survive over 200 shots even with considerable postpulse energy. The average of a large number of shots showed that with a 7-kG magnetic field in the anode-cathode gap, the current density is consistent with the Child-Langmuir proton prediction if the effective gap spacing is taken as 0.43 cm at 50 nsec and 0.25 cm at 100 nsec. This is in good agreement with predictions of the effective spacing from the time history of diode perveance. Ion current densities were found to increase by about a factor of 2 going from a diode voltage of 200 to 300 kV. As an example of maximum parameters, by using the half-length anode (1100 cm^2) at $B/B^* = 2-3$, total currents exceeding 100 kA were obtained at 100 nsec with a diode voltage of about 200 kV. The total ion current could be estimated by averaging the probe signals and extrapolating over the diode area. Between 50 and 100 nsec in the pulse, the efficiency (I_i/I_e) was found to be 0.60 ± 0.15 , consistent with the perveance measurement.

Knowing the diode current density, the propagation characteristics of the beam can be predicted if three quantities are known: $\Delta\alpha_z$, the axial-divergence half-angle; $\Delta\alpha_r$, the radial-divergence half-angle; and, α , the magnetic deflection of the protons crossing the acceleration gap. The axial divergence was found to be $\Delta\alpha_z = 3.2 \pm 0.4^\circ$ from inspection of the beam expansion as it emerged from a slot with use of grazing-angle witness plates. The ability to trace indications of the slot pattern almost to the axis indicates that the space-charge imbalance must be less than 3%. It should be noted that the propagation region is at high vacuum (less than 5×10^{-5} Torr) so the negative space charge must be supplied by cold electrons extracted from the cathode surfaces. The predicted variation of the axial distribution with radius is shown in Fig. 3(a). The deflection from the normal of a proton crossing the magnetically insulated gap is given by α

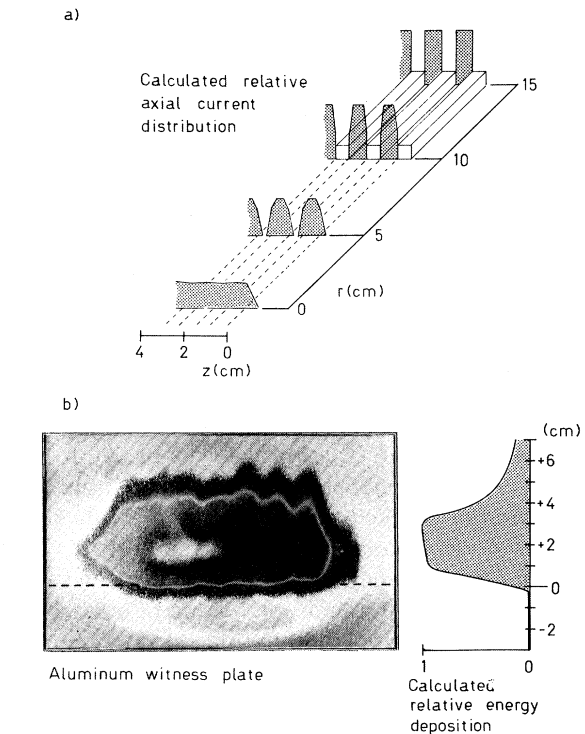


FIG. 3. Beam propagation in cathode plenum. All data are plotted on the same scale. (a) Axial distribution of protons as a function of radius for $\Delta\alpha_z = 3^\circ$. (b) Actual witness plate, displayed with predicted time-integrated energy-deposition profile for $\Delta\alpha_r = 6^\circ$.

$= 1.7(m_e/m_p)^{1/2} B/B^*$. The numerical factor is due to an enhancement brought about by field lines diffusing into the surface of the exclusion cathode. Figure 3(b) shows the pattern of damage produced by a shot on an aluminum plate located on a diameter of the system. The maximum-damage location agreed well with the predicted proton deflection (typically about 5°). For a given radial-divergence angle, with knowledge of α , and under the assumption that ions are emitted uniformly in the azimuth, it is possible to predict the energy-deposition profile on the witness plate. This is plotted in Fig. 3(b) for a choice of $\Delta\alpha_r = 6^\circ$. The radial-divergence angle can be measured quantitatively by locating a detector of known acceptance angle ($\pm 45^\circ$ in this case) near the focus as shown, recording the effective current density, and using the known diode current density with the axial variation shown in Fig. 3(a). If this is done, $\Delta\alpha_r$ is found to be $6.2 \pm 1.2^\circ$. The maximum current density measured in this way was approximately 320 A/cm^2 , giving a radial-compression factor of 10. Detectors located at intermediate radii (3.3 and 7.7 cm)

gave signals that were within 15% of the prediction made using the axial behavior of Fig. 3(a) and a R_d/r law for the current density. The rather poor divergence angles obtained in this experiment are probably due to the coarse plasma surface on the anode. With the geometry in question, it would be expected that the radial divergence would be greater than the axial divergence.

The major result of these initial investigations is that intense ion beams can be controlled geometrically and that propagation in a high vacuum, field free region to a first-order focus is governed by single particle trajectories with no evidence of space charge effects. Although the focused current density was not as high as we had hoped, the problems involved appear amenable to solution. We plan to optimize the system with the following modifications:

(a) Plasma sources localized over the slots will be used to maximize the total system efficiency to keep the diode voltage up while extracting a large number of protons into the propagation volume. (b) The capacitive division of the plasma anode in azimuth will be considerably increased, reducing the radial divergence angle. (c) Experiments will be performed using a weak negative bias magnetic field inside the propagation volume. If the total flux inside the anode is zero, all protons, independent of the diode voltage, will arrive at the axis in the absence of radial divergence. In this case, neutralizing electrons will be supplied axially along field lines,

as in previous work.^{1,11}

This work was supported by Sandia Laboratories and the Office of Naval Research.

¹S. Humphries, R. N. Sudan, and L. Wiley, *J. Appl. Phys.* **47**, 2382 (1976).

²P. Dreike, C. Eichenberger, S. Humphries, and R. N. Sudan, *J. Appl. Phys.* **47**, 85 (1976).

³F. Winterberg, *Plasma Phys.* **17**, 69 (1975).

⁴M. J. Clauser, *Phys. Rev. Lett.* **35**, 848 (1975).

⁵A. W. Maschke, *Bull. Am. Phys. Soc.* **21**, 1060 (1976).

⁶H. I. Milde and N. W. Harris, in *Proceedings of the Thirteenth Symposium on Electron, Ion and Photon Beam Technology*, edited by R. F. W. Pease and J. G. Skinner (American Institute of Physics, New York, 1975), p. 1188.

⁷In order to make a large-area plasma by surface electrical breakdown, a sheet of hydrocarbon insulator backed by a metal anode is divided by an array of metal pins inserted into the insulator and flush with its outer surface. Electrical breakdown is initiated on application of the pulsed diode voltage at the pins by fringing fields, and the surface surrounding each pin is capacitively coupled to the cathode.

⁸For a discussion of the theory of these probes at high ion-current density, see C. Eichenberger, S. Humphries, J. Maenchen, and R. N. Sudan, to be published.

⁹R. N. Sudan and R. V. Lovelace, *Phys. Rev. Lett.* **31**, 1174 (1973).

¹⁰K. D. Bergeron, *Appl. Phys. Lett.* **28**, 306 (1976).

¹¹S. Humphries, C. Eichenberger, and R. N. Sudan, to be published.

Experimental Observation of Explosive Instability Due to a Helical Electron Beam^(a)

R. Sugaya, M. Sugawa, and H. Nomoto

Department of Physics, Faculty of Science, Ehime University, Matsuyama, Japan

(Received 9 February 1977)

We have performed experiments on explosive instability of space-charge waves of the helical electron beam due to nonlinear wave-particle interaction. The fast and slow beam modes interact nonlinearly with the helical electron beam and grow simultaneously.

Explosive instability is one of the most interesting phenomena in nonlinear plasma theory,^{1,2} but experimental results supporting such theory have been lacking.³ Further, an experimental study on explosive instability due to nonlinear wave-particle interaction (nonlinear Landau damping) has yet to be reported, although the experimental investigations of the nonlinear Landau damping of nonexplosive type have been given by many authors.⁴⁻⁶ In this Letter, we report the experimen-

tal observation of the explosive instability due to the nonlinear Landau damping.

For an electron beam-plasma system in a magnetic field, the resonant condition for nonlinear wave-particle interaction of two waves with the electron beam is given by^{4,6}

$$\omega_1 - \omega_2 - (k_{\parallel 1} - k_{\parallel 2})v_b = m\omega_c, \quad (1)$$

where v_b is the velocity of the beam, ω_c the electron cyclotron frequency, m an integer, and the

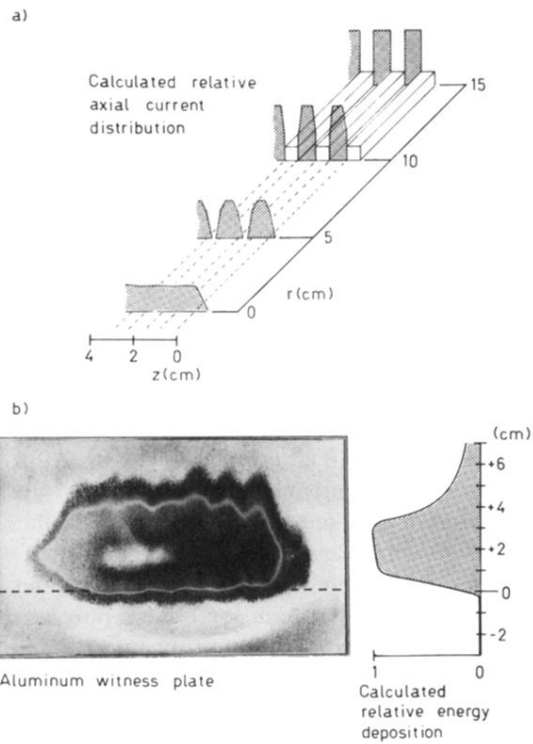


FIG. 3. Beam propagation in cathode plenum. All data are plotted on the same scale. (a) Axial distribution of protons as a function of radius for $\Delta\alpha_z = 3^\circ$. (b) Actual witness plate, displayed with predicted time-integrated energy-deposition profile for $\Delta\alpha_r = 6^\circ$.